

# Probing the goldstino excitation via tunneling current noise in a Bose-Fermi mixture

Tingyu Zhang<sup>1,2,\*</sup>

<sup>1</sup>*Department of Physics, School of Science, The University of Tokyo, Tokyo 113-0033, Japan*

<sup>2</sup>*Interdisciplinary Theoretical and Mathematical Sciences Program (iTHEMS), RIKEN, Wako 351-0198, Japan*

The Goldstino, which is a fermionic Nambu-Goldstone mode, has been predicted in a Bose-Fermi mixture when the supersymmetry is broken. To detect this excitation mode, we theoretically investigate the shot noise of the supersymmetry-like tunneling current in a repulsively interacting ultracold Bose-Fermi mixture. The Fano factor, which is defined by the noise-to-current ratio, reflects the elementary carriers of the tunneling process. The change of the Fano factor microscopically as the density changes evinces a crossover from the quasiparticle transport to multiparticle (Goldstino) transport. The tunneling channel can also be changed by tuning the potential barrier.

## I. INTRODUCTION

The Ultracold atoms have become a unique tool to study the nature of quantum many-body systems owing to their cleanliness and high experimental flexibility. The well-developed experimental techniques for cold atoms enable exploration of various regimes including weakly interacting Bose-Einstein condensates [1–3], the superfluid-Mott insulator transition [4, 5] for bosonic systems, and the crossover between the Bardeen-Cooper-Schrieffer (BCS) and Bose-Einstein condensation (BEC) regimes [6–8], as well as the itinerant ferromagnetic transition [9] for the case of fermions.

The realization of mixtures of bosonic and fermionic quantum fluids [10–12] has opened new avenues for investigating quantum many-body systems, where the components obey different statistical rules and interact with each other [13–15]. The interspecies interaction allows the sympathetic cooling [10, 11, 16–18], and can change the dynamics in each component [19]. Issues in the study of Bose-Fermi mixtures include their stability and miscibility [15, 20–26], transport properties [27–29], and the possible applications in quantum simulations to achieve supersymmetry [30–37]. The supersymmetry, which assigns a superpartner (a particle with the same mass but opposite statistics) to each elementary particle, appears to be broken when there is an explicit mass or chemical potential imbalance between the two components. The symmetry breaking leads to the emergence of a massless fermionic Nambu-Goldstone mode, referred to as a Goldstino [30, 38–40]. The Goldstino has garnered significant research interest, as it carries a fermionic quantum number, unlike most collective modes in cold atom systems, yet shares many similarities with the more familiar Nambu-Goldstone boson. [41, 42]. Beyond cold atomic systems, a fermionic mode linked to spontaneous supersymmetry breaking is also predicted in quark-gluon plasmas at extremely high temperatures [43, 44]. In spite of its importance for understanding the supersymmetry, the existence of Goldstino remains elusive and has yet to be observed. However, it has been found that Goldstino

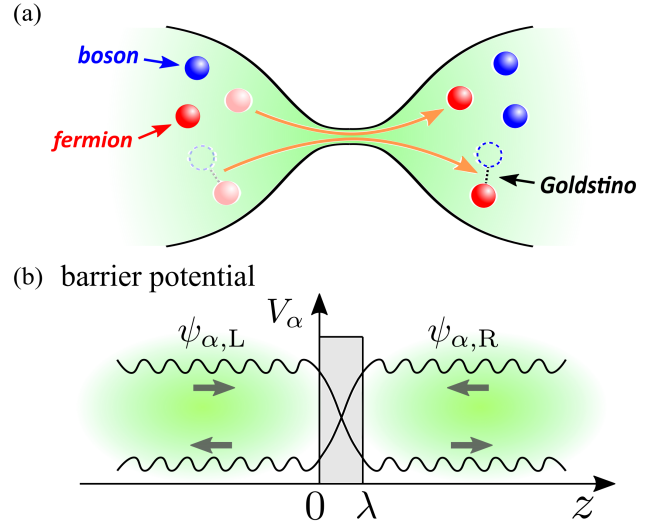


FIG. 1. (a) Schematic view of the two-terminal system we study. Chemical potential bias between two reservoirs provokes quasiparticle as well as supercharge tunnelings. The dashed circle represents the hole, and the pair of a fermion and a bosonic hole denotes a Goldstino. (b) Rectangular potential barrier with height  $V_\alpha$  ( $\alpha = b$  for bosons and  $\alpha = f$  for fermions) and width  $\lambda$  applied for the junction.  $\psi_{\alpha,L(R)}$  denotes wave functions of particles in the left (right) reservoir.

excitations can contribute to the tunneling transport as a multiparticle process in an ultracold Bose-Fermi mixture [29], and thus could be detected through tunneling signals. One challenge, however, is to distinguish the signal of Goldstino from those of quasiparticle processes.

Out of consideration for this, we propose detecting the Goldstino excitation through the shot noise of the supersymmetry-like tunneling current. Quantum shot noise arises from the discrete nature of current carriers, and is therefore proportional to both the effective charge and the average current [45]. In solid state systems, shot noise has been used to probe the fractional charges in the fractional quantum Hall regime [46, 47] and the effective spin associated with magnon tunneling through a ferromagnet-insulator-normal metal interface [48]. It

\* zhangty@g.ecc.u-tokyo.ac.jp

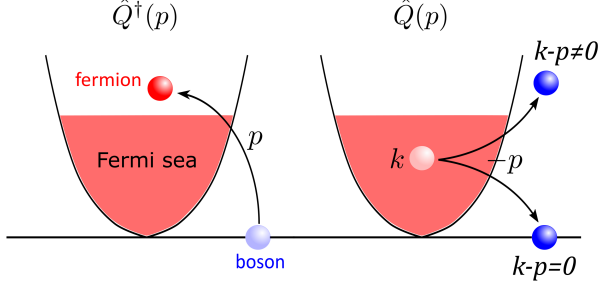


FIG. 2. The supercharge operators. The left process represents  $\hat{Q}^\dagger$ , which converts a boson into a fermion, while the right one represents  $\hat{Q}$ , converting a fermion into a boson. The black line at the bottom represents the condensate of bosons.

is also shown recently that in cold atomic systems the shot noise can serve as a probe of multiparticle processes [49, 50], revealing a crossover from the quasiparticle transport to multiparticle transport as the interaction strength is tuned by using Feshbach resonances [51]. In our work, we focus on a small mass-balanced mixture,  $^{173}\text{Yb}$ - $^{174}\text{Yb}$ , where Feshbach resonances are not applicable. Instead, we analyze the tunneling channel by tuning the particle densities and the shape of the potential barrier. Once the Goldstino tunneling channel is identified, it could provide the evidence for the existence of supersymmetry in such Bose-Fermi mixtures.

This paper is structured as follows: In Sec. II, we introduce the Hamiltonian of a two terminal model. In Sec. III, we derived the formulas of the supersymmetry-like tunneling current and shot noise up to leading order. In Sec. IV, we analyze the Fano factor for supersymmetry-like transport and show the numerical results with changing particle densities and barrier potentials. The conclusion and perspectives are given in Sec. V.

Throughout the paper, we take  $\hbar = k_B = 1$  and the volumes of both reservoirs to be unity.

## II. FORMALISM

We consider a two-terminal model for mixtures of ultracold Bose and Fermi gases, where particles in one reservoir have a probability of tunneling through a barrier potential to the other side, as depicted in Fig. 1 (a). In this setup, the bosons predominantly exist in the BEC phase with zero momentum below the BEC critical temperature, while the fermions occupy a fully filled Fermi sea. We assume the gas is homogeneous within each reservoir, far from the barrier, allowing the wave functions to be asymptotically treated as plane waves. Then the effective Hamiltonian of the total system can be given as  $\hat{H} = \hat{H}_L + \hat{H}_R + \hat{H}_{1t} + \hat{H}_{2t}$  [29], where the reservoir

Hamiltonian reads

$$\begin{aligned} \hat{H}_{i=L,R} = & \sum_{\mathbf{k}} \varepsilon_{\mathbf{k},f} \hat{f}_{\mathbf{k},i}^\dagger \hat{f}_{\mathbf{k},i} + \sum_{\mathbf{k}} \varepsilon_{\mathbf{k},b} \hat{b}_{\mathbf{k},i}^\dagger \hat{b}_{\mathbf{k},i} \\ & + \frac{U_{bb}}{2} \sum_{\mathbf{P},\mathbf{q},\mathbf{q}'} \hat{b}_{\frac{\mathbf{P}}{2}+\mathbf{q},i}^\dagger \hat{b}_{\frac{\mathbf{P}}{2}-\mathbf{q},i}^\dagger \hat{b}_{\frac{\mathbf{P}}{2}-\mathbf{q}',i} \hat{b}_{\frac{\mathbf{P}}{2}+\mathbf{q}',i} \\ & + U_{bf} \sum_{\mathbf{P},\mathbf{q},\mathbf{q}'} \hat{b}_{\frac{\mathbf{P}}{2}+\mathbf{q},i}^\dagger \hat{f}_{\frac{\mathbf{P}}{2}-\mathbf{q},i}^\dagger \hat{f}_{\frac{\mathbf{P}}{2}-\mathbf{q}',i} \hat{b}_{\frac{\mathbf{P}}{2}+\mathbf{q}',i}. \end{aligned} \quad (1)$$

Here  $\hat{f}(\hat{b})$  denotes the fermionic (bosonic) annihilation operator, and  $\varepsilon_{\mathbf{p},\alpha=b,f} = p^2/(2m_\alpha)$  is the kinetic energy of particles.  $U_{bb}$  and  $U_{bf}$  are, respectively, the coupling strengths for the boson-boson and boson-fermion interactions, which are characterized by the scattering lengths  $a_{bb}$  and  $a_{bf}$  as  $U_{bb} = (4\pi a_{bb})/m_b$  and  $U_{bf} = (2\pi a_{bf})/m_r$ , with  $m_r = 1/(1/m_b + 1/m_f)$  denoting the reduced mass. Notice that the fermion-fermion interaction disappears since we consider a polarized Fermi gas. For the tunneling Hamiltonian, we divide it into one-body ( $\hat{H}_{1t}$ ) and two-body ( $\hat{H}_{2t}$ ) terms, where the one-body term is given by

$$\begin{aligned} \hat{H}_{1t} = & \sum_{\mathbf{p},\mathbf{q}} \mathcal{T}_{f,\mathbf{p},\mathbf{q}} [\hat{f}_{\mathbf{p},L}^\dagger \hat{f}_{\mathbf{q},R} + \hat{f}_{\mathbf{p},R}^\dagger \hat{f}_{\mathbf{q},L}] \\ & + \sum_{\mathbf{p},\mathbf{q}} \mathcal{T}_{b,\mathbf{p},\mathbf{q}} [\hat{b}_{\mathbf{p},L}^\dagger \hat{b}_{\mathbf{q},R} + \hat{b}_{\mathbf{p},R}^\dagger \hat{b}_{\mathbf{q},L}]. \end{aligned} \quad (2)$$

We apply rectangular potential barriers with width  $\lambda$  and height  $V_\alpha$  ( $V_f$  for fermions and  $V_b$  for bosons) as shown in Fig 1 (b). Then the one-body tunneling amplitude  $\mathcal{T}_{\alpha,\mathbf{k},\mathbf{k}'}$  can be approximately given by (see Appendix A)

$$\mathcal{T}_{\alpha,\mathbf{p},\mathbf{q}} \simeq T_{\alpha,\mathbf{q}} \delta_{p_z,q_z} \epsilon_q + V_\alpha \mathcal{C}_{\alpha,p_z,q_z}, \quad (3)$$

where we omit the Hartree terms  $\frac{U_{fb}}{2} \sum_i \hat{N}_{b,\mathbf{p}-\mathbf{q},i}$ ,  $\frac{U_{bb}}{2} \sum_i \hat{N}_{b,\mathbf{p}-\mathbf{q},i}$ , and  $\frac{U_{fb}}{2} \sum_i \hat{N}_{f,\mathbf{p}-\mathbf{q},i}$ , which are negligible due to the short-range interaction. Here  $p_z$  is the  $z$  component of momentum  $\mathbf{p}$ ,  $T_{\alpha,\mathbf{p}}$  is the single-particle transmission coefficient through the barrier, and  $\mathcal{C}_{\alpha,p_z,q_z}$  represents the overlap of wave functions within the potential barrier.

The two-body tunneling Hamiltonian includes three parts:  $\hat{H}_{2t} = \hat{H}_{bb} + \hat{H}_{bf} + \hat{H}_Q$ , respectively corresponding to contributions of boson-boson pairs, boson-fermion pairs and the supercharges. By defining the annihilation operators for boson-boson and boson-fermion pairs:  $\hat{P}_{bb,i}(\mathbf{p}) = \sum_{\mathbf{k}} \hat{b}_{-\mathbf{k}+\mathbf{p}/2,i} \hat{b}_{\mathbf{k}+\mathbf{p}/2,i}$  and  $\hat{P}_{bf,i}(\mathbf{p}) = \sum_{\mathbf{k}} \hat{b}_{-\mathbf{k}+\mathbf{p}/2,i} \hat{f}_{\mathbf{k}+\mathbf{p}/2,i}$ , the pair tunneling terms can be written as

$$\hat{H}_{bb} = \frac{1}{2} \mathcal{G}_{bb} \sum_{\mathbf{p},\mathbf{q}} [\hat{P}_{bb,L}^\dagger(\mathbf{p}) \hat{P}_{bb,R}(\mathbf{q}) + \text{H.c.}], \quad (4a)$$

$$\hat{H}_{bf} = \mathcal{G}_{bf} \sum_{\mathbf{p},\mathbf{q}} [\hat{P}_{bf,L}^\dagger(\mathbf{p}) \hat{P}_{bf,R}(\mathbf{q}) + \text{H.c.}], \quad (4b)$$

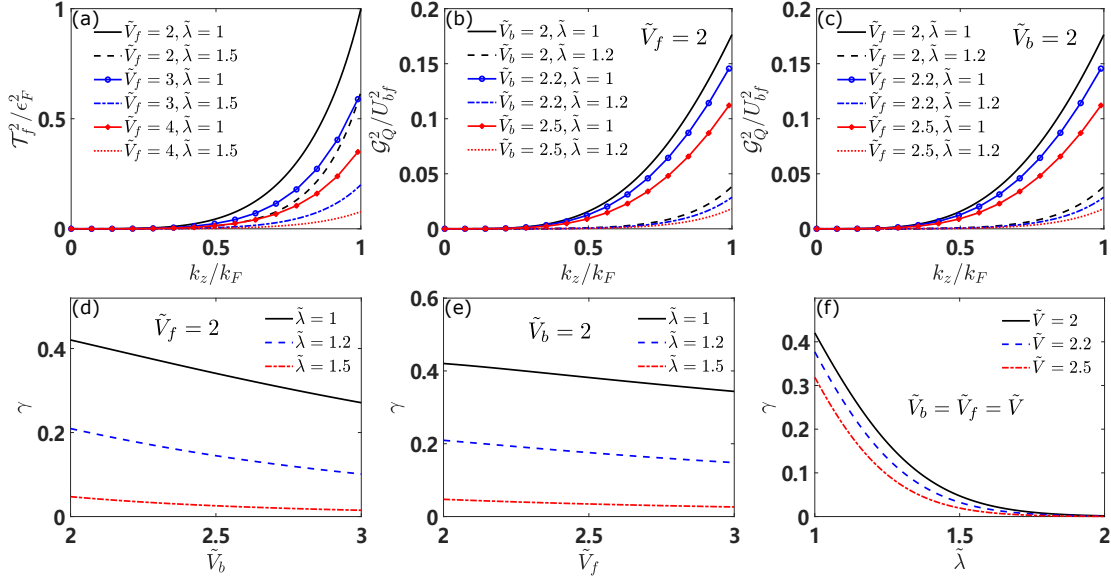


FIG. 3. Upper panels: Momentum dependence of (a) module squared fermionic quasiparticle tunneling strengths, (b) module squared supercharge tunneling strengths with different  $\tilde{V}_b$ , and (c) module squared supercharge tunneling strengths with different  $\tilde{V}_f$ . Lower panels: values of  $\gamma = \epsilon_F \mathcal{G}_Q / (U_{bf} \mathcal{T}_f)$  with changing (d) height of bosonic barrier, (e) height of fermionic barrier, and (f) width of barriers. Here  $\tilde{V}_\alpha = V_\alpha / \epsilon_F$  and  $\tilde{\lambda} = \lambda k_F$ .

The pair tunneling amplitude  $\mathcal{G}_{bb}$  and  $\mathcal{G}_{bf}$  can be expressed as  $\mathcal{G}_{bb} = U_{bb} \text{Re}[T_{b,0}^2]$ ,  $\mathcal{G}_{bf} = U_{bf} \text{Re}[T_{b,0} T_{f,0}]$  by taking the long-wavelength limit. The supercharge tunneling term is given by

$$H_Q = \mathcal{G}_Q \sum_{\mathbf{p}, \mathbf{q}} \left[ \hat{Q}_L^\dagger(\mathbf{p}) \hat{Q}_R(\mathbf{q}) + \text{H.c.} \right]. \quad (5)$$

Here  $\hat{Q}$  is the supercharge annihilation operator defined by

$$\hat{Q}_i(\mathbf{p}) = \sum_{\mathbf{k}} \hat{f}_{\mathbf{k},i} \hat{b}_{\mathbf{k}-\mathbf{p},i}^\dagger, \quad (6)$$

which satisfy the anticommutation relation and therefore is a fermionic operator. Physically this operator annihilates a fermion while creating a boson with momentum transferred, as shown in Fig. 2. The tunneling amplitude  $\mathcal{G}_Q$ , within the long-wavelength limit, can be given by  $\mathcal{G}_Q = U_{bf} \text{Re}[T_{b,0} T_{f,0}^*]$ .

The supersymmetry-like current operator yields  $\hat{I}_{\text{SUSY}} = i[\hat{N}_{b,L} - \hat{N}_{f,L}, \hat{H}]$ , where  $\hat{N}_{f,i} = \sum_{\mathbf{k}} \hat{f}_{\mathbf{k},i}^\dagger \hat{f}_{\mathbf{k},i}$  and  $\hat{N}_{b,i} = \sum_{\mathbf{k}} \hat{b}_{\mathbf{k},i}^\dagger \hat{b}_{\mathbf{k},i}$  represent particle number densities of fermions and bosons, respectively. In order to facilitate the identification of Goldstino current, we consider the same bosonic chemical potential but different fermionic chemical potentials in the two reservoirs, such that the supercharge tunneling can be induced while the bosonic quasiparticle and boson-boson pair tunneling do not occur. On the other hand we focus on weakly boson-fermion interacting regime where the two-body boundary state is so deep that the boson-fermion pair tunneling process

is suppressed. Thus the remaining contributions come from the fermionic quasiparticle and supercharge, whose current operators read

$$\hat{I}_{1t} = i \sum_{\mathbf{p}, \mathbf{q}} \left[ \mathcal{T}_f (\hat{f}_{\mathbf{p},R}^\dagger \hat{f}_{\mathbf{q},L} - \hat{f}_{\mathbf{p},L}^\dagger \hat{f}_{\mathbf{q},R}) \right], \quad (7)$$

$$\hat{I}_Q = 2i \mathcal{G}_Q \sum_{\mathbf{p}, \mathbf{q}} \hat{Q}_L^\dagger(\mathbf{p}) \hat{Q}_R(\mathbf{q}) + \text{H.c.} \quad (8)$$

The momentum dependence of their tunneling strengths is depicted in Figs. 3 (a), (b), and (c), where  $\epsilon_F$  and  $k_F$  are Fermi energy and Fermi momentum of the Fermi gas in the left reservoir. It is shown that  $\mathcal{G}_Q$  is more sensitive than  $\mathcal{T}_f$  to the shape of potential barrier. To compare the two tunneling strengths more intuitively, we define the ratio  $\gamma = \epsilon_F \mathcal{G}_Q / (U_{bf} \mathcal{T}_f)$ . Figs. 3 (d), (e), and (f) exhibit how this ratio is affected by the height and width of the potential barrier. The details of calculation can be checked in Appendix A.

### III. SUPERSYMMETRY-LIKE CURRENT AND NOISE

By expanding the formulas of tunneling currents up to the leading order within the Schwinger-Keldysh Green's function approach [52, 53], and using the Langreth rule,

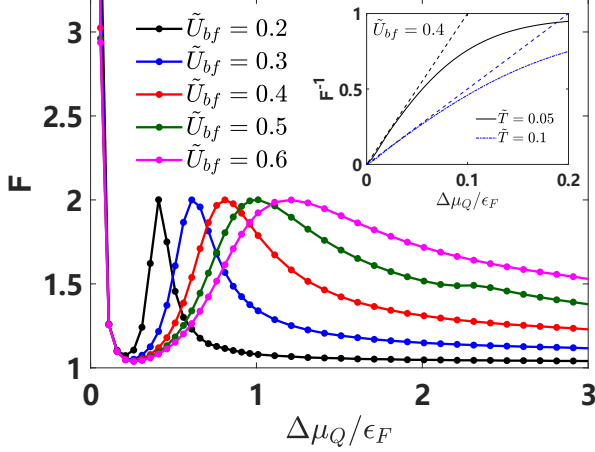


FIG. 4. Bias dependence of the Fano factor for the supersymmetry-like transport in a  $^{173}\text{Yb}$ - $^{174}\text{Yb}$  ultracold mixture, where  $\tilde{U}_{bf} = N_f U_{bf} / \epsilon_F = 4k_F a_{bf} / (3\pi)$ . We take  $\gamma = 0.25$ . Ratio between bosonic and fermionic densities is set to be  $N_b / N_f = 2$ . The Onsager's relation  $F^{-1}(\Delta\mu_Q \rightarrow 0) = \Delta\mu_Q / 2T$  is shown in the inset, where we define  $\tilde{T} = T / T_F$ , with  $T_F$  denoting the Fermi temperature.

we obtain the leading-order formulas of the currents:

$$I_{1t} = 4\mathcal{T}_f^2 \int \frac{d\omega}{2\pi} \sum_{\mathbf{p}, \mathbf{q}} \text{Im} G_{f,\mathbf{p},L}(\omega - \Delta\mu_f) \text{Im} G_{f,\mathbf{q},R}(\omega) \times [f_f(\omega - \Delta\mu_f) - f_f(\omega)], \quad (9)$$

$$I_Q = 8\mathcal{G}_Q^2 \sum_{\mathbf{p}, \mathbf{q}} \int \frac{d\Omega}{2\pi} \text{Im} \chi_{\mathbf{p},L}(\Omega - \Delta\mu_Q) \text{Im} \chi_{\mathbf{q},R}(\Omega) \times [f_f(\Omega - \Delta\mu_Q) - f_f(\Omega)], \quad (10)$$

where  $\Delta\mu_f = \mu_{f,L} - \mu_{f,R}$  is the fermionic chemical potential bias,  $\mu_{Q,i} = \mu_{f,i} - \mu_{b,i}$ ,  $\Delta\mu_Q = \mu_{Q,L} - \mu_{Q,R}$ , and  $f_f(\omega) = 1/e^{\omega/T} + 1$  is the Fermi distribution function.  $G_{f,\mathbf{p},i}$  is the retarded single-particle Green's function and  $\chi$  is the retarded Goldstino propagator, which is defined as  $\chi_{\mathbf{p}}(t, t') = i\theta(t - t') \langle \{\hat{Q}_{\mathbf{p}}(t), \hat{Q}_{\mathbf{p}}^\dagger(t')\} \rangle$  in the time representation. The Goldstino propagator can be calculated, by using the random phase approximation (RPA) [29, 36, 37], as

$$\chi_{\mathbf{p}}(\Omega) = \frac{\Pi_{\mathbf{p}}(\Omega)}{1 + U_{bf} \Pi_{\mathbf{p}}(\Omega)}, \quad (11)$$

with  $\Pi_{\mathbf{p}}(\Omega)$  denoting the one-loop diagram, namely, the non-interacting Goldstino propagator. We can see from Fig. 2 that  $\Pi_{\mathbf{p}}(\Omega)$  includes the contribution of both the condensate and the bosons with non-zero momentum. We can thus write  $\Pi_{\mathbf{p}}$  as the sum of two parts:  $\Pi_{\mathbf{p}} = \Pi_{\mathbf{p}}^b + \Pi_{\mathbf{p}}^c$ , with

$$\Pi_{\mathbf{p}}^b(\Omega) = -\frac{N_b^0}{\Omega + \epsilon_F + i\delta - \mathbf{p}^2/2m}, \quad (12)$$

$$\Pi_{\mathbf{p}}^c(\Omega) = -\int \frac{d^3\mathbf{k}}{(2\pi)^3} \frac{f_f(\xi_{\mathbf{k}+\mathbf{p},f}) + f_b(\xi_{\mathbf{k},b})}{\Omega + i\delta - \xi_{\mathbf{k}+\mathbf{p},f} + \xi_{\mathbf{k},b}}, \quad (13)$$

where  $N_b^0$  denotes the number of bosons in the condensate state, and  $f_b(\omega)$  denotes the distribution function of bosons out of the condensate. Eq. (12) is the contribution of condensate bosons, leading to a series of poles at  $\Omega + \epsilon_F - \mathbf{p}^2/2m = 0$  in the Goldstino spectrum. In contrast, Eq. (13) arises from the boson with non-zero momentum, resulting in the continuum of the spectrum [29, 36]. At extremely low temperatures, almost all bosons are distributed in the BEC condensate, implying  $N_b^0 \rightarrow N_b$  and  $f_b(\xi_{\mathbf{k},b}) \rightarrow 0$ .

Now we introduce the current shot noise, which is defined as  $\hat{\mathcal{S}}(t_1, t_2) = \frac{1}{2} \langle \hat{I}(t_1) \hat{I}(t_2) + \hat{I}(t_2) \hat{I}(t_1) \rangle$  [54, 55], where the quantum average  $\langle \dots \rangle$  represents quantum average with respect to the unperturbed state of the system. For the supersymmetry-like current we have  $\hat{\mathcal{S}}_{\text{SUSY}} = \hat{\mathcal{S}}_{1t} + \hat{\mathcal{S}}_Q$ , corresponding to the one-body and Goldstino transport processes, respectively. Its Fourier decomposition reads

$$\mathcal{S}(\omega) = \frac{1}{\tau} \int_0^\tau dt_1 \int_0^\tau dt_2 e^{i\omega(t_1 - t_2)} \mathcal{S}(t_1, t_2), \quad (14)$$

where  $\tau$  is the typical time scale for the noise measurement and should be much larger than the transport time scale [56]. Here we simply take the limit  $\tau \rightarrow \infty$  and the dc-limit of noise:  $\mathcal{S} := \mathcal{S}(\omega \rightarrow 0)$ . With the truncation up to the first order, we obtain the following expressions:

$$\begin{aligned} \mathcal{S}_{1t} = & 4\mathcal{T}_f^2 \sum_{\mathbf{p}, \mathbf{q}} \int \frac{d\omega}{2\pi} \text{Im} G_{f,\mathbf{q},L}(\omega - \Delta\mu_f) \text{Im} G_{f,\mathbf{p},R}(\omega) \\ & \times [f_f(\omega - \Delta\mu_f)(1 - f_f(\omega)) + (1 - f_f(\omega - \Delta\mu_f))f_f(\omega)], \end{aligned} \quad (15)$$

$$\begin{aligned} \mathcal{S}_Q = & 16\mathcal{G}_Q^2 \sum_{\mathbf{p}, \mathbf{q}} \int \frac{d\omega}{2\pi} \text{Im} \chi_{\mathbf{p},L}(\omega - \Delta\mu_Q) \text{Im} \chi_{\mathbf{q},R}(\omega) \\ & \times [f_f(\omega - \Delta\mu_Q)(1 - f_f(\omega)) + (1 - f_f(\omega - \Delta\mu_Q))f_f(\omega)]. \end{aligned} \quad (16)$$

Compared Eqs. (15), (16) with Eqs. (9), (10), one can easily find that at large bias limit ( $\Delta\mu_f \rightarrow 0$  and  $\Delta\mu_Q \rightarrow 0$ ), we have  $\mathcal{S}_{1s}/I_{1s} = 1$  and  $\mathcal{S}_{2s}/I_{2s} = 2$ . This indicates that the value of the ratio  $(\mathcal{S}_{1s} + \mathcal{S}_{2s})/(I_{1s} + I_{2s})$  lies between 1 and 2, and can reflect the ratio of two types of charge carriers.

#### IV. FANO FACTOR

To investigate the tunneling channel of the supersymmetry-like transport, we define the Fano factor as  $F = (\mathcal{S}_{1s} + \mathcal{S}_{2s})/(I_{1s} + I_{2s})$ , which is a useful probe for the current carrier. We consider the



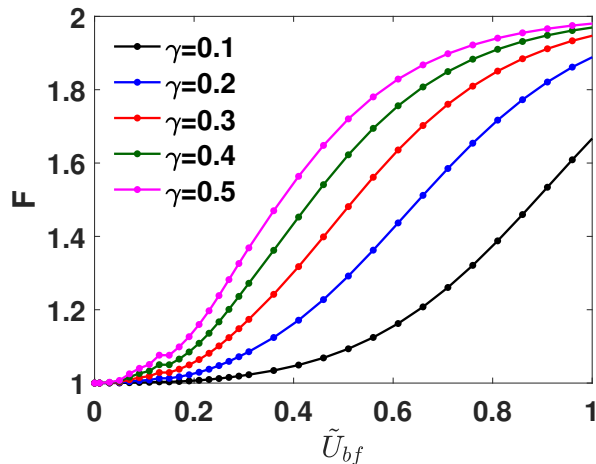


FIG. 5. Interaction dependence of the Fano factor for the supersymmetry-like transport with different values of  $\gamma$  in a  $^{173}\text{Yb}$ - $^{174}\text{Yb}$  ultracold mixture. We take  $\Delta\mu_Q/\epsilon_F = 3$  to maintain the large bias limit. Ratio between bosonic and fermionic densities is set to be  $N_b/N_f = 2$ .

$^{173}\text{Yb}$ - $^{174}\text{Yb}$  mixture [57, 58] as the context, where the boson-fermion and boson-boson scattering lengths are experimentally determined as  $a_{bf} = 138.49a_0$  and  $a_{bb} = 104.72a_0$  [59] ( $a_0$  is the Bohr radius). By setting the Fermi energy and the density of fermions of the left reservoir to  $\epsilon_F$  and  $N_f$ , and tuning the chemical potential of fermions in the right side, we analyze the bias dependence of the Fano factor as shown in Fig. 4, where we define the dimensionless interaction strength  $\tilde{U}_{bf} = N_f U_{bf}/\epsilon_F = 4k_F a_{bf}/(3\pi)$ , and fix the ratio of densities of two components as  $N_b/N_f = 2$ . We note that although the scattering lengths can not be adjusted through magnetic Feshbach resonances, we can tune the  $\tilde{U}_{bf}$  by changing the  $k_F$ , namely the particle density of fermions. Fig. 4 demonstrates the validity of large bias limit when  $\Delta\mu_Q$  reaches a relatively large value, such as  $\Delta\mu_Q/\epsilon_F = 3$ . In addition, a divergence appears at  $\Delta\mu_Q \rightarrow 0$ , resulting from zero current but finite noise. The inset figure shows the Onsager's relation near  $\Delta\mu_Q = 0$ , which yields  $F^{-1} = \Delta\mu_Q/2T$ .

Fig. 5 shows the Fano factor as a function of the dimensionless interaction strength  $\tilde{U}_{bf}$  in the  $^{173}\text{Yb}$ - $^{174}\text{Yb}$  ultracold mixture where particle densities are varied while keeping the ratio  $N_b/N_f = 2$  fixed. We focus on the weakly coupling regime to avoid the instability toward pair formation [60, 61] and phase separation [62] in the strongly repulsively interacting regime. We set  $\Delta\mu_Q/\epsilon_F = 3$  for satisfying the large-bias limit, which can be justified according to Fig. 4. We see that the Fano factor gradually changes from 1 to a value close to 2 with increasing  $\tilde{U}_{bf}$ , indicating a crossover from fermionic quasiparticle tunneling ( $F = 1$ ) to Goldstino tunneling ( $F = 2$ ). Similar phenomenon has also been found in the BCS-BEC crossover regime [49] and repulsively interacting Fermi gases [50], where the current carrier changes

from quasiparticles to pairs and magnon modes, respectively. It is also worth noting that the interaction dependence of  $F$  is deeply related to the value of  $\gamma$ , which is characterized by the property of the junction barrier, which indicates that the tunneling channel can be tuned by adjusting the potential barrier.

Although the results in this work are specified for the  $^{173}\text{Yb}$ - $^{174}\text{Yb}$  superfluid mixture, our approach is applicable for other Bose-Fermi mixtures with small mass imbalances, including  $^6\text{Li}$ - $^7\text{Li}$  [12, 63],  $^{39}\text{K}$ - $^{40}\text{K}$  [64],  $^{40}\text{K}$ - $^{41}\text{K}$  [65],  $^{84}\text{Sr}$ - $^{87}\text{Sr}$  [59],  $^{87}\text{Rb}$ - $^{87}\text{Sr}$  [66], and  $^{161}\text{Dy}$ - $^{162}\text{Dy}$  [67]. Moreover, Feshbach resonances allow tuning the interspecies scattering lengths in some of these mixtures [65, 66], offering a more flexible experimental platform to study the effects of interspecies interactions on the tunneling channels and Goldstino spectral properties. A noise measurement experiment for density current in cold atoms has been proposed with a two-terminal system [68], where one reservoir overlaps with a single-sided optical cavity, and a probe beam monitors the atom number in this reservoir. The current noise can be measured through the phase of the probe, which gives a real-time measurement of the atom number. Such method might also be applicable for the supersymmetry-like tunneling in the Bose-Fermi mixture, where the number of bosons and fermions should be measured respectively.

## V. CONCLUSION

In this study, we theoretically investigate the tunneling transport induced by chemical potential bias and the corresponding shot noise in an ultracold Bose-Fermi mixture with explicit supersymmetry breaking. We show how the shot noise can serve as a probe of the current carrier at large bias limit. The Fano factor, defined as the noise-to-current ratio, takes the value 1 at noninteracting case, indicating quasiparticles dominant the tunneling process. As the density of atoms increases, the Fano factor changes to a value close to 2, signifying a transition to Goldstino-dominated tunneling. Furthermore, we show that the tunneling channel can be controlled by adjusting the junction barrier, which could facilitate experimental investigations of supercharge tunneling transport. Our approach offers a novel method for detecting the Goldstino in mixtures of bosonic and fermionic atoms and may also prove useful for exploring Nambu-Goldstone fermions in other condensed matter systems with supersymmetric properties [69–71].

## ACKNOWLEDGMENTS

T. Z. thanks Hiroyuki Tajima and Haozhao Liang for useful discussions. T. Z. was supported by the RIKEN Junior Research Associate Program.

### Appendix A: Calculation of tunneling coupling strengths

In this appendix, we show the details of our calculation of tunneling coupling strengths  $\mathcal{T}_f$  and  $\mathcal{G}_Q$ , as well as the ratio  $\gamma$ . We consider a rectangular barrier potential:

$$V_\alpha(z) = \begin{cases} V_\alpha & 0 < z < \lambda \\ 0 & z \leq 0, z \geq \lambda \end{cases} \quad (\text{A1})$$

Here we consider a particle from the left reservoir ( $z < 0$ ) to the right reservoir ( $z \geq \lambda$ ) described by  $\Psi_{\alpha,\mathbf{k},\text{L}}(\mathbf{r}) = e^{i\mathbf{k}_\perp \cdot \mathbf{r}_\perp} \psi_{\alpha,k_z,\text{L}}(z)$  where  $\mathbf{r}_\perp = (x, y)$  and  $\mathbf{k}_\perp = (k_x, k_y)$  are the position and momentum vectors perpendicular to the barrier, respectively. According to the behavior of a wave function passing through a potential barrier,  $\psi_{k_z,\text{L}}(z)$  for a particle coming from the left reservoir can be written as

$$\psi_{\alpha,k_z,\text{L}}(z) = \begin{cases} e^{ik_z z} + R_\alpha e^{-ik_z z} & z \leq 0, \\ C_{1\alpha} e^{\kappa_{z\alpha} z} + C_{2\alpha} e^{-\kappa_{z\alpha} z} & 0 < z < \lambda, \\ T_\alpha e^{ik_z z} & z \geq \lambda. \end{cases} \quad (\text{A2})$$

where  $\kappa_{z\alpha} = \sqrt{2mV_\alpha - k_z^2}$  is a real number (we suppose the potential barrier is larger than the particle's kinetic energy). According to the continuity of  $\psi(z)$  and  $d\psi(z)/dz$  at the boundary of barrier  $z = 0$  and  $z = \lambda$ , the reflection coefficient  $R$  and transmission coefficient  $T$  should be

$$R_{\alpha,\mathbf{k}} = \frac{2(\kappa_{z\alpha}^2 + k_z^2) \sinh(\kappa_{z\alpha} \lambda)}{(\kappa_{z\alpha} + ik_z)^2 e^{-\kappa_{z\alpha} \lambda} - (\kappa_{z\alpha} - ik_z)^2 e^{\kappa_{z\alpha} \lambda}}, \quad (\text{A3})$$

$$T_{\alpha,\mathbf{k}} = \frac{4ik_z \kappa_{z\alpha} e^{-ik_z \lambda}}{(\kappa_{z\alpha} + ik_z)^2 e^{-\kappa_{z\alpha} \lambda} - (\kappa_{z\alpha} - ik_z)^2 e^{\kappa_{z\alpha} \lambda}}, \quad (\text{A4})$$

while the coefficients  $C_{1\alpha,\mathbf{k}}$  and  $C_{2\alpha,\mathbf{k}}$  for the wave function inside the potential barrier are obtained as

$$C_{1\alpha,\mathbf{k}} = \frac{i2k_z(\kappa_{z\alpha} + ik_z)e^{-\kappa_{z\alpha} \lambda}}{(\kappa_{z\alpha} + ik_z)^2 e^{-\kappa_{z\alpha} \lambda} - (\kappa_{z\alpha} - ik_z)^2 e^{\kappa_{z\alpha} \lambda}}, \quad (\text{A5})$$

$$C_{2\alpha,\mathbf{k}} = \frac{i2k_z(\kappa_{z\alpha} - ik_z)e^{\kappa_{z\alpha} \lambda}}{(\kappa_{z\alpha} + ik_z)^2 e^{-\kappa_{z\alpha} \lambda} - (\kappa_{z\alpha} - ik_z)^2 e^{\kappa_{z\alpha} \lambda}}. \quad (\text{A6})$$

We may obtain the wave function  $\Psi_{\alpha,\mathbf{k},\text{R}}(\mathbf{r})$  of a particle coming from the right reservoir to the left one in a same way:

$$\psi_{\alpha,-k_z,\text{R}}(z) = \begin{cases} T'_\alpha e^{-ik_z z} & z \geq \lambda \\ C'_{1\alpha} e^{\kappa_{z\alpha} z} + C'_{2\alpha} e^{-\kappa_{z\alpha} z} & 0 < z < \lambda, \\ e^{-ik_z z} + R'_\alpha e^{ik_z z}, & z \leq 0 \end{cases} \quad (\text{A7})$$

where we have the relations:  $R'_{\alpha,-\mathbf{k}} = e^{-i2k_z \lambda} R_{\alpha,\mathbf{k}}$ ,  $C'_{1\alpha,-\mathbf{k}} = e^{-(\kappa_{z\alpha} + ik_z)\lambda} C_{2\alpha,\mathbf{k}}$ ,  $C'_{2\alpha,-\mathbf{k}} = e^{(\kappa_{z\alpha} - ik_z)\lambda} C_{1\alpha,\mathbf{k}}$ , and  $T'_{\alpha,-\mathbf{k}} = T_{\alpha,\mathbf{k}}$ .

The total Hamiltonian of the system is given by

$$\begin{aligned} \hat{H} = & \sum_{\alpha=f,b} \int d^3\mathbf{r} \hat{\psi}_\alpha^\dagger(\mathbf{r}) \left[ -\frac{\nabla^2}{2m_\alpha} + V_\alpha(\mathbf{r}) \right] \hat{\psi}_\alpha(\mathbf{r}) \\ & + \frac{U_{bb}}{2} \int d^3\mathbf{r} \hat{\psi}_b^\dagger(\mathbf{r}) \hat{\psi}_b^\dagger(\mathbf{r}) \hat{\psi}_b(\mathbf{r}) \hat{\psi}_b(\mathbf{r}) \\ & + U_{bf} \int d^3\mathbf{r} \hat{\psi}_b^\dagger(\mathbf{r}) \hat{\psi}_b(\mathbf{r}) \hat{\psi}_f^\dagger(\mathbf{r}) \hat{\psi}_f(\mathbf{r}), \end{aligned} \quad (\text{A8})$$

For the steady-state transport between two reservoirs, the field operator can be decomposed as

$$\hat{\psi}_\alpha(\mathbf{r}) = \hat{\psi}_{\alpha,\text{L}}(\mathbf{r}) + \hat{\psi}_{\alpha,\text{R}}(\mathbf{r}). \quad (\text{A9})$$

We expand the operator  $\hat{\Psi}_\alpha, i(\mathbf{r})$  with respect to the asymptotic wave functions as

$$\hat{\psi}_{f,i}(\mathbf{r}) = \sum_{\mathbf{k}} \psi_{\mathbf{k},f,i}(\mathbf{r}) \hat{f}_{\mathbf{k},i}, \quad (\text{A10})$$

$$\hat{\psi}_{b,i}(\mathbf{r}) = \sum_{\mathbf{k}} \psi_{\mathbf{k},b,i}(\mathbf{r}) \hat{b}_{\mathbf{k},i}, \quad (\text{A11})$$

where we only use wave functions  $z < 0$  and  $z > \lambda$ , since we characterize the tunneling strength by using the asymptotic wave functions far away from the tunnel barrier. Substituting them to the total Hamiltonian and supposing  $\mathbf{k}_\perp$  of the particle before and after tunneling to be unchanged, we can write the momentum-dependent tunneling strength as

$$\mathcal{T}_{f,\mathbf{k},\mathbf{k}'} \simeq T_{f,\mathbf{k}'} \delta_{k_z,k'_z} \epsilon_{k'} + V_f \mathcal{C}_{f,k_z,k'_z}. \quad (\text{A12})$$

For  $\mathcal{T}_{f,\mathbf{k},\mathbf{k}'}$  we omit the Hartree term  $\frac{U_{fb}}{2} \sum_i \hat{N}_{b,\mathbf{k}_1-\mathbf{k}_2,i}$  which is negligible due to the short-range interaction, while

$$\mathcal{C}_{f,k_z,k'_z} = \frac{1}{\lambda} \int_0^\lambda dz \psi_{f,k_z,\text{R}}^\dagger(z) \psi_{f,k'_z,\text{L}}(z). \quad (\text{A13})$$

Here  $\epsilon_k = k^2/(2m)$  denotes the particle's kinetic energy. Now we assume that  $\mathbf{k} - \mathbf{k}' \rightarrow 0$ , and Eq. (A13) can be approximately written as

$$\mathcal{C}_{f,k_z} \simeq - \frac{\sinh(\kappa_{zf}\lambda)}{\lambda\kappa_{zf}} \frac{4k_z^2(\kappa_{zf}^2 + k_z^2)e^{-ik_z\lambda}}{[(\kappa_{zf} + ik_z)^2 e^{-\kappa_{zf}\lambda} - (\kappa_{zf} - ik_z)^2 e^{\kappa_{zf}\lambda}]^2} - \frac{8k_z^2 e^{-ik_z\lambda} [(\kappa_{zf}^2 - k_z^2) \cosh(\kappa_{zf}\lambda) - i2\kappa_{zf}k_z \sinh(\kappa_{zf}\lambda)]}{[(\kappa_{zf} + ik_z)^2 e^{-\kappa_{zf}\lambda} - (\kappa_{zf} - ik_z)^2 e^{\kappa_{zf}\lambda}]^2}. \quad (\text{A14})$$

Then the fermionic one-body tunneling strength becomes

$$\mathcal{T}_{f,\mathbf{k}} \simeq T_{f,\mathbf{k}} \epsilon_k + V_f \mathcal{C}_{f,k_z}. \quad (\text{A15})$$

Simliar we can obtain the goldstino tunneling coupling

strength as

$$\mathcal{G}_Q = U_{bf} \text{Re} [T_{b,\mathbf{k}} T_{f,\mathbf{k}}^*]. \quad (\text{A16})$$

According to Eq. (A4), we have

$$\text{Re}[T_{\alpha,\mathbf{k}}] = \frac{4k_z^2 \kappa_{z\alpha}^2 \cos(k_z\lambda) \cosh(\kappa_{z\alpha}\lambda) - 2k_z \kappa_{z\alpha} (\kappa_{z\alpha}^2 - k_z^2) \sin(k_z\lambda) \sinh(\kappa_{z\alpha}\lambda)}{(\kappa_{z\alpha}^2 - k_z^2)^2 \sinh^2(\kappa_{z\alpha}\lambda) + 4\kappa_{z\alpha}^2 k_z^2 \cosh^2(\kappa_{z\alpha}\lambda)}, \quad (\text{A17})$$

$$\text{Im}[T_{\alpha,\mathbf{k}}] = - \frac{2k_z \kappa_{z\alpha} (\kappa_{z\alpha}^2 - k_z^2) \cos(k_z\lambda) \sinh(\kappa_{z\alpha}\lambda) + 4k_z^2 \kappa_{z\alpha}^2 \sin(k_z\lambda) \cosh(\kappa_{z\alpha}\lambda)}{(\kappa_{z\alpha}^2 - k_z^2)^2 \sinh^2(\kappa_{z\alpha}\lambda) + 4\kappa_{z\alpha}^2 k_z^2 \cosh^2(\kappa_{z\alpha}\lambda)}. \quad (\text{A18})$$

Then the Goldstino tunneling strength can be calculated as

$$\frac{\mathcal{G}_Q}{U_{bf}} = \text{Re}[T_{b,\mathbf{k}}] \text{Re}[T_{f,\mathbf{k}}] + \text{Im}[T_{b,\mathbf{k}}] \text{Im}[T_{f,\mathbf{k}}]. \quad (\text{A19})$$

- 
- [1] E. A. Cornell and C. E. Wieman, Nobel lecture: Bose-einstein condensation in a dilute gas, the first 70 years and some recent experiments, *Rev. Mod. Phys.* **74**, 875 (2002).
  - [2] A. L. Fetter, Rotating trapped bose-einstein condensates, *Rev. Mod. Phys.* **81**, 647 (2009).
  - [3] D. C. Aveline, J. R. Williams, E. R. Elliott, C. Dutenhofer, J. R. Kellogg, J. M. Kohel, N. E. Lay, K. Oudrhiri, R. F. Shotwell, N. Yu, *et al.*, Observation of bose-einstein condensates in an earth-orbiting research lab, *Nature* **582**, 193 (2020).
  - [4] M. Greiner, O. Mandel, T. Esslinger, T. W. Hänsch, and I. Bloch, Quantum phase transition from a superfluid to a mott insulator in a gas of ultracold atoms, *nature* **415**, 39 (2002).
  - [5] C.-L. Hung, X. Zhang, N. Gemelke, and C. Chin, Slow mass transport and statistical evolution of an atomic gas across the superfluid-mott-insulator transition, *Phys. Rev. Lett.* **104**, 160403 (2010).
  - [6] C. A. Regal, M. Greiner, and D. S. Jin, Observation of resonance condensation of fermionic atom pairs, *Phys. Rev. Lett.* **92**, 040403 (2004).
  - [7] M. Bartenstein, A. Altmeyer, S. Riedl, S. Jochim, C. Chin, J. H. Denschlag, and R. Grimm, Crossover from a molecular bose-einstein condensate to a degenerate fermi gas, *Phys. Rev. Lett.* **92**, 120401 (2004).
  - [8] W. Zwerger, *The BCS-BEC Crossover and the Unitary Fermi Gas*, 1st ed., Vol. 836 (Springer, Berlin, Heidelberg, 2012).
  - [9] G.-B. Jo, Y.-R. Lee, J.-H. Choi, C. A. Christensen, T. H. Kim, J. H. Thywissen, D. E. Pritchard, and W. Ketterle, Itinerant ferromagnetism in a fermi gas of ultracold atoms, *Science* **325**, 1521 (2009).
  - [10] F. Schreck, L. Khaykovich, K. L. Corwin, G. Ferrari, T. Bourdel, J. Cubizolles, and C. Salomon, Quasipure bose-einstein condensate immersed in a fermi sea, *Phys. Rev. Lett.* **87**, 080403 (2001).
  - [11] A. G. Truscott, K. E. Strecker, W. I. McAlexander, G. B. Partridge, and R. G. Hulet, Observation of fermi pressure in a gas of trapped atoms, *Science* **291**, 2570 (2001).
  - [12] I. Ferrier-Barbut, M. Delehaye, S. Laurent, A. T. Grier, M. Pierce, B. S. Rem, F. Chevy, and C. Salomon, A mixture of bose and fermi superfluids, *Science* **345**, 1035 (2014).
  - [13] K. K. Das, Bose-fermi mixtures in one dimension, *Phys. Rev. Lett.* **90**, 170403 (2003).
  - [14] M. Lewenstein, L. Santos, M. A. Baranov, and H. Fehrmann, Atomic bose-fermi mixtures in an optical lattice, *Phys. Rev. Lett.* **92**, 050401 (2004).

- [15] K. Günter, T. Stöferle, H. Moritz, M. Köhl, and T. Esslinger, Bose-fermi mixtures in a three-dimensional optical lattice, *Phys. Rev. Lett.* **96**, 180402 (2006).
- [16] C. J. Myatt, E. A. Burt, R. W. Ghrist, E. A. Cornell, and C. E. Wieman, Production of two overlapping bose-einstein condensates by sympathetic cooling, *Phys. Rev. Lett.* **78**, 586 (1997).
- [17] F. Schreck, G. Ferrari, K. L. Corwin, J. Cubizolles, L. Khaykovich, M.-O. Mewes, and C. Salomon, Sympathetic cooling of bosonic and fermionic lithium gases towards quantum degeneracy, *Phys. Rev. A* **64**, 011402 (2001).
- [18] Y. Chen, M. Horikoshi, M. Kuwata-Gonokami, and K. Yoshioka, Creating a noninteracting bose gas in equilibrium at finite temperature, *Phys. Rev. A* **105**, 043312 (2022).
- [19] K. Patel, G. Cai, H. Ando, and C. Chin, Sound propagation in a bose-fermi mixture: From weak to strong interactions, *Phys. Rev. Lett.* **131**, 083003 (2023).
- [20] K. Mølmer, Bose condensates and fermi gases at zero temperature, *Phys. Rev. Lett.* **80**, 1804 (1998).
- [21] F. M. Marchetti, C. J. M. Mathy, D. A. Huse, and M. M. Parish, Phase separation and collapse in bose-fermi mixtures with a feshbach resonance, *Phys. Rev. B* **78**, 134517 (2008).
- [22] Z.-Q. Yu, S. Zhang, and H. Zhai, Stability condition of a strongly interacting boson-fermion mixture across an interspecies feshbach resonance, *Phys. Rev. A* **83**, 041603 (2011).
- [23] G. Bertaina, E. Fratini, S. Giorgini, and P. Pieri, Quantum monte carlo study of a resonant bose-fermi mixture, *Phys. Rev. Lett.* **110**, 115303 (2013).
- [24] R. S. Lous, I. Fritsche, M. Jag, F. Lehmann, E. Kirilov, B. Huang, and R. Grimm, Probing the interface of a phase-separated state in a repulsive bose-fermi mixture, *Phys. Rev. Lett.* **120**, 243403 (2018).
- [25] K. Manabe and Y. Ohashi, Thermodynamic stability, compressibility matrices, and effects of mediated interactions in a strongly interacting bose-fermi mixture, *Phys. Rev. A* **103**, 063317 (2021).
- [26] X. Shen, N. Davidson, G. M. Bruun, M. Sun, and Z. Wu, Strongly interacting bose-fermi mixtures: Mediated interaction, phase diagram, and sound propagation, *Phys. Rev. Lett.* **132**, 033401 (2024).
- [27] P.-T. Qi and W.-S. Duan, Tunneling dynamics and phase transition of a bose-fermi mixture in a double well, *Phys. Rev. A* **84**, 033627 (2011).
- [28] S. Wang, X. Yin, Y.-Y. Chen, Y. Zhang, and X.-W. Guan, Emergent ballistic transport of bose-fermi mixtures in one dimension, *Journal of Physics A: Mathematical and Theoretical* **53**, 464002 (2020).
- [29] T. Zhang, Y. Guo, H. Tajima, and H. Liang, Probing the goldstino excitation through tunneling transport in a bose-fermi mixture with explicitly broken supersymmetry, *Phys. Rev. B* **110**, 064512 (2024).
- [30] Y. Yu and K. Yang, Supersymmetry and the goldstino-like mode in bose-fermi mixtures, *Phys. Rev. Lett.* **100**, 090404 (2008).
- [31] T. Shi, Y. Yu, and C. P. Sun, Supersymmetric response of a bose-fermi mixture to photoassociation, *Phys. Rev. A* **81**, 011604 (2010).
- [32] H.-H. Lai and K. Yang, Relaxation of a goldstino-like mode due to supersymmetry breaking in bose-fermi mixtures, *Phys. Rev. A* **91**, 063620 (2015).
- [33] J.-P. Blaizot, Y. Hidaka, and D. Satow, Spectral properties of the goldstino in supersymmetric bose-fermi mixtures, *Phys. Rev. A* **92**, 063629 (2015).
- [34] B. Bradlyn and A. Gromov, Supersymmetric waves in bose-fermi mixtures, *Phys. Rev. A* **93**, 033642 (2016).
- [35] N. Sannomiya, H. Katsura, and Y. Nakayama, Supersymmetry breaking and nambu-goldstone fermions in an extended nicolai model, *Phys. Rev. D* **94**, 045014 (2016).
- [36] J.-P. Blaizot, Y. Hidaka, and D. Satow, Goldstino in supersymmetric bose-fermi mixtures in the presence of a bose-einstein condensate, *Phys. Rev. A* **96**, 063617 (2017).
- [37] H. Tajima, Y. Hidaka, and D. Satow, Goldstino spectrum in an ultracold bose-fermi mixture with explicitly broken supersymmetry, *Phys. Rev. Res.* **3**, 013035 (2021).
- [38] A. Salam and J. Strathdee, On goldstone fermions, *Physics Letters B* **49**, 465 (1974).
- [39] E. Witten, Dynamical breaking of supersymmetry, *Nuclear Physics B* **188**, 513 (1981).
- [40] V. Lebedev and A. Smilga, Supersymmetric sound, *Nuclear Physics B* **318**, 669 (1989).
- [41] Y. Nambu and G. Jona-Lasinio, Dynamical model of elementary particles based on an analogy with superconductivity. i, *Phys. Rev.* **122**, 345 (1961).
- [42] J. Goldstone, Field theories with superconductor solutions, *Il Nuovo Cimento (1955-1965)* **19**, 154 (1961).
- [43] Y. Hidaka, D. Satow, and T. Kunihiro, Ultrasoft fermionic modes at high temperature, *Nuclear Physics A* **876**, 93 (2012).
- [44] D. Satow, Ultrasoft fermion mode and off-diagonal boltzmann equation in a quark-gluon plasma at high temperature, *Phys. Rev. D* **87**, 096011 (2013).
- [45] Y. Blanter and M. Büttiker, Shot noise in mesoscopic conductors, *Physics Reports* **336**, 1 (2000).
- [46] L. Saminadayar, D. C. Glatthli, Y. Jin, and B. Etienne, Observation of the  $e/3$  fractionally charged Laughlin quasiparticle, *Phys. Rev. Lett.* **79**, 2526 (1997).
- [47] R. de Picciotto, M. Reznikov, M. Heiblum, V. Umansky, G. Bunin, and D. Mahalu, Direct observation of a fractional charge, *Physica B: Condensed Matter* **249-251**, 395 (1998).
- [48] M. Matsuo, Y. Ohnuma, T. Kato, and S. Maekawa, Spin current noise of the spin seebeck effect and spin pumping, *Phys. Rev. Lett.* **120**, 037201 (2018).
- [49] H. Tajima, D. Oue, M. Matsuo, and T. Kato, Nonequilibrium noise as a probe of pair-tunneling transport in the BCS-BEC crossover, *PNAS Nexus* **2**, pgad045 (2023).
- [50] T. Zhang, H. Tajima, and H. Liang, Magnonic spin-current shot noise in an itinerant fermi gas, *Phys. Rev. Appl.* **21**, L031001 (2024).
- [51] X. Yin, R. Grimm, P. Julienne, and E. Tiesinga, Feshbach resonances in ultracold gases, *Rev. Mod. Phys.* **82**, 1225 (2010).
- [52] J. Schwinger, Brownian motion of a quantum oscillator, *Journal of Mathematical Physics* **2**, 407 (1961).
- [53] L. V. Keldysh, Diagram technique for nonequilibrium processes, *Zh. Eksp. Teor. Fiz.* **47**, 1515 (1964).
- [54] M. Büttiker, Scattering theory of current and intensity noise correlations in conductors and wave guides, *Phys. Rev. B* **46**, 12485 (1992).
- [55] O. S. Lumbroso, L. Simine, A. Nitzan, D. Segal, and O. Tal, Electronic noise due to temperature differences in atomic-scale junctions, *Nature* **562**, 240 (2018).
- [56] J.-P. Brantut, C. Grenier, J. Meineke, D. Stadler,



- S. Krinner, C. Kollath, T. Esslinger, and A. Georges, A thermoelectric heat engine with ultracold atoms, *Science* **342**, 713 (2013).
- [57] T. Fukuhara, S. Sugawa, Y. Takasu, and Y. Takahashi, All-optical formation of quantum degenerate mixtures, *Phys. Rev. A* **79**, 021601 (2009).
- [58] S. Sugawa, K. Inaba, S. Taie, R. Yamazaki, M. Yamashita, and Y. Takahashi, Interaction and filling-induced quantum phases of dual mott insulators of bosons and fermions, *Nature Physics* **7**, 642 (2011).
- [59] M. K. Tey, S. Stellmer, R. Grimm, and F. Schreck, Double-degenerate bose-fermi mixture of strontium, *Phys. Rev. A* **82**, 011608 (2010).
- [60] P. Massignan, M. Zaccanti, and G. M. Bruun, Polarons, dressed molecules and itinerant ferromagnetism in ultracold fermi gases, *Reports on Progress in Physics* **77**, 034401 (2014).
- [61] Y. Ji, G. L. Schumacher, G. G. T. Assumpção, J. Chen, J. T. Mäkinen, F. J. Vivanco, and N. Navon, Stability of the repulsive fermi gas with contact interactions, *Phys. Rev. Lett.* **129**, 203402 (2022).
- [62] A. Amico, F. Scazza, G. Valtolina, P. E. S. Tavares, W. Ketterle, M. Inguscio, G. Roati, and M. Zaccanti, Time-resolved observation of competing attractive and repulsive short-range correlations in strongly interacting fermi gases, *Phys. Rev. Lett.* **121**, 253602 (2018).
- [63] S. Laurent, M. Pierce, M. Delehay, T. Yefsah, F. Chevy, and C. Salomon, Connecting few-body inelastic decay to quantum correlations in a many-body system: A weakly coupled impurity in a resonant fermi gas, *Phys. Rev. Lett.* **118**, 103403 (2017).
- [64] S. Falke, H. Knöckel, J. Friebe, M. Riedmann, E. Tiemann, and C. Lisdat, Potassium ground-state scattering parameters and born-oppenheimer potentials from molecular spectroscopy, *Phys. Rev. A* **78**, 012503 (2008).
- [65] C.-H. Wu, I. Santiago, J. W. Park, P. Ahmadi, and M. W. Zwierlein, Strongly interacting isotopic bose-fermi mixture immersed in a fermi sea, *Phys. Rev. A* **84**, 011601 (2011).
- [66] V. Barbé, A. Ciamei, B. Pasquiou, L. Reichsöllner, F. Schreck, P. S. Żuchowski, and J. M. Hutson, Observation of feshbach resonances between alkali and closed-shell atoms, *Nature Physics* **14**, 881 (2018).
- [67] K. Maeda, G. Baym, and T. Hatsuda, Simulating dense qcd matter with ultracold atomic boson-fermion mixtures, *Phys. Rev. Lett.* **103**, 085301 (2009).
- [68] S. Uchino, M. Ueda, and J.-P. Brantut, Universal noise in continuous transport measurements of interacting fermions, *Phys. Rev. A* **98**, 063619 (2018).
- [69] N. Sannomiya and H. Katsura, Supersymmetry breaking and nambu-goldstone fermions in interacting majorana chains, *Phys. Rev. D* **99**, 045002 (2019).
- [70] P. Marra, D. Inotani, and M. Nitta, 1d majorana goldstinos and partial supersymmetry breaking in quantum wires, *Communications Physics* **5**, 149 (2022).
- [71] U. Miura and K. Totsuka, Supersymmetry breaking in a generalized nicolai model with fermion (2023), arXiv:2308.03346 [cond-mat.str-el].